Radiation Physics and Chemistry 223 (2024) 111926

Contents lists available at ScienceDirect

Radiation Physics and Chemistry

journal homepage: www.elsevier.com/locate/radphyschem

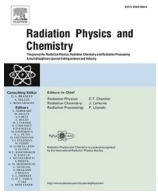

Dosimetric parameters and radiation tolerance of epitaxial diodes for diagnostic radiology and computed tomography beams

JosemaryA.C. Gonçalves [a], Alessio Mangiarotti [b], Patrícia L. Antonio [a], LindaV.E. Caldas [a], CarmenC. Bueno [a,*]

[a] Instituto de Pesquisas Energéticas e Nucleares, Comissão Nacional de Energia Nuclear – IPEN/CNEN, 05508-000, São Paulo, Brazil
[b] Instituto de Física - Universidade de São Paulo, IFUSP, 05508-080, São Paulo, Brazil

ARTICLE INFO

Handling Editor: Dr. Chris Chantler

Keywords:
Diagnostic radiology beam dosimetry
Computed tomography beam dosimetry
Si PIN photodiode dosimeter
X-ray dosimetry

ABSTRACT

A custom-made EPI diode-based dosimetry system is thoroughly characterized for diagnostic radiology and computed tomography beams. The diode has a thin n-type epitaxial layer (50 μm) grown on a thick (300 μm) Czochralski silicon substrate. It operates as an online radiation dosimeter in the short-circuit current mode. In this case, the key dosimetric quantity is the dose rate, correlated with the output current from the diode exposed to radiation. The corresponding collected charge (the integral of the current signal) is proportional to the dose. Irradiations are performed with the Pantak-Seifert 160HS Isovolt X-ray generator previously standardized by Radcal RC6-RD and RC3-CT ionization chambers. The data gathered with all radiation quality beams confirm the linearity with dose and dose rate despite a slight energy dependence. Independently from the beam energy, the dosimetric parameters of repeatability (<0.3%), long-term stability (0.4%/year), angular response (<3%, ± 5°), dose rate dependence (<3%), and signal-to-noise ratio (≥4900) fully adhere to the IEC 61674 recommendations. Compliance with the accumulated dose stability requirement (1.0%/40 Gy) is almost achieved with the pristine diode and effectively accomplished through radiation conditioning with ^{60}Co gamma rays. Under the latter condition, the lifespan of the diode can easily reach 15 kGy, assuring the high reusability of this diode for diagnostic radiology and computed tomography dosimetry before requiring recalibrations.

1. Introduction

Semiconductor detectors, mostly based on diodes, transistors, and diamonds have been increasingly used as relative dosimeters in radiation protection, medical imaging, and radiation therapy (Kumar et al., 2014; Damulira et al., 2019; Jursinic, 2019). Ionization chambers are well-established gold standard reference dosimeters essential for ensuring dose accuracy and calibration of semiconductor dosimeters. These, in turn, have sensitivities orders of magnitude higher than ionization chambers, which is advantageous in applications where spatial resolution is the main concern. Interest in these applications has driven the development of new transistor manufacturing technologies, particularly MOSFETs, and synthetic diamonds with characteristics similar to natural ones and better cost-effectiveness (Rosenfeld, 2002, 2016; Damulira et al., 2019; Pettinato et al., 2023).

Silicon diodes have been widely applied for electron and photon beam dosimetry, covering broad dose and dose rate ranges (Khoury et al., 1999; Grusell and Medin, 2000; Griessbach et al., 2005; Rosenfeld, 2007; Oliveira et al., 2016; Jursinic, 2023). Usually, the diode operates in the short-circuit current mode and remains unbiased to minimize the dark current contribution to the radiation-induced current signal. The dosimetric parameter is the net output current that is, within certain limits, linearly dependent on the dose rate. The corresponding collected charge (obtained as the integral of the current signal) is proportional to the dose. Many articles in the literature report several advantages of diode-based dosimeters, yet a key drawback is also well known: a sensitivity decay with increasing accumulated doses. The trend of this decay is characterized by a very fast current decrease when the irradiation starts, followed by a gradually slower drop as the diode accumulates larger doses (Rikner and Grussel, 1983; Lindström et al., 1999; Pini et al., 2003; Casati et al., 2005; Bruzzi et al., 2007). The physical phenomena underlying this decrease in sensitivity are associated with radiation-induced defects (mainly the creation of generation-recombination centers) in the Si bulk and how they affect the

* Corresponding author. Av. Prof. Lineu Prestes 2242, Cidade Universitária, 05508-000, São Paulo, SP, Brazil.
E-mail address: ccbueno@ipen.br (CarmenC. Bueno).

https://doi.org/10.1016/j.radphyschem.2024.111926
Received 27 February 2024; Received in revised form 5 June 2024; Accepted 8 June 2024
Available online 13 June 2024

active volume of the unbiased diode (Liao et al., 2024). Under this operating mode, the active volume is mostly determined by the minority carrier diffusion length, which shortens with increasing accumulated doses. When the diffusion length decreases below the thickness of the diode, the active volume and then the sensitivity start to decrease drastically (Gonçalves et al., 2020).

Three experimental approaches are adopted to overcome this difficulty: i) Pre-irradiating the diode to introduce many radiation damage defects that mitigate the relative change of the diffusion length. It has been accomplished with commercially available silicon diodes, although less sensitive and slightly dependent on temperature and dose rate (for pulsed beams) (Barthe, 2001). ii) Choosing thin diodes with thicknesses smaller than the lowest minority carrier diffusion length anticipated at the foreseen accumulated dose. This strategy has been validated with thin optical sensors, which feature low dark currents, high stability, and a very small temperature coefficient (Jursinic, 2023). Reliable results have been obtained with thin photodiodes, but a less pronounced decay is still observed when applied for low-dose radiation processing applications (Gonçalves et al., 2021, 2022). iii) Using diodes with enhanced radiation tolerance, also called radiation hard diodes, specially developed in high-energy physics research programs to withstand harsh irradiation (Candelori, 2006; Lindström et al., 2006; Fretwurst et al., 2007; Härkönen et al., 2007; Hönniger et al., 2007; Camargo et al., 2007; Moll, 2018; Bueno et al., 2022). This issue has been tackled using two strategies: developing devices with different geometries (thickness, guard rings, implanted junctions) and tailoring the concentration of the impurities in the silicon material processed through different techniques. A combined approach of these strategies has been adopted to produce epitaxial diodes with distinct structures and physical characteristics (Kemmer et al., 2005). Feasibility studies on applying EPI diodes as dosimeters have been reported in the literature (Bruzzi et al., 2007; Santos et al., 2011; Aldosari et al., 2013; Gonçalves et al., 2014).

The EPI diode investigated in this work has a thin n-type epitaxial layer (25 μm–75 μm) grown on a thick (300 μm–500 μm) Czochralski silicon substrate with a high oxygen concentration. The p-n junction is provided by a highly doped p-type silicon layer (≅ 1 μm) on the front side of the diode. This structure, which keeps the active volume constant with less dark current, is the uttermost characteristic of the diode regarding its outstanding radiation hardness (Lindström et al., 2006; Bruzzi et al., 2007; Fretwurst et al., 2007; Aldosari et al., 2013). This work aims to study the dosimetric response and the radiation tolerance of EPI diodes for diagnostic radiology and computed tomography X-rays to take advantage of their thin structure, low dark current, and negligible entrance dead layer, suitable for low-energy photon detection. A dosimetric characterization is thoroughly performed in compliance with the internationally accepted recommendations for diode-based dosimeters in standard diagnostic beam dosimetry.

2. Materials and methods

2.1. Diode and dosimetry probe

The starting material of the diode investigated in this work consists of an n-type epitaxial silicon layer (50 μm thick; resistivity of 50 Ω cm) produced by ITME (Poland) using a highly Sb doped n-type Czochralski (Cz) silicon wafer (300 μm thick; resistivity of 0.02 Ω cm). Pad diodes (25 mm^2 active area) are processed by CiS (Germany) in a p^+-n-n^+ structure with a p^+ electrode attained through B implantation to a depth of 0.6 μm into the epitaxial layer. The Cz substrate is the backside n^{++} ohmic contact, with an area of 1 cm^2 given by the outer dimension of the device. More details about the processing technique and diode characteristics can be found elsewhere (Lindströem et al., 2006; Hönniger

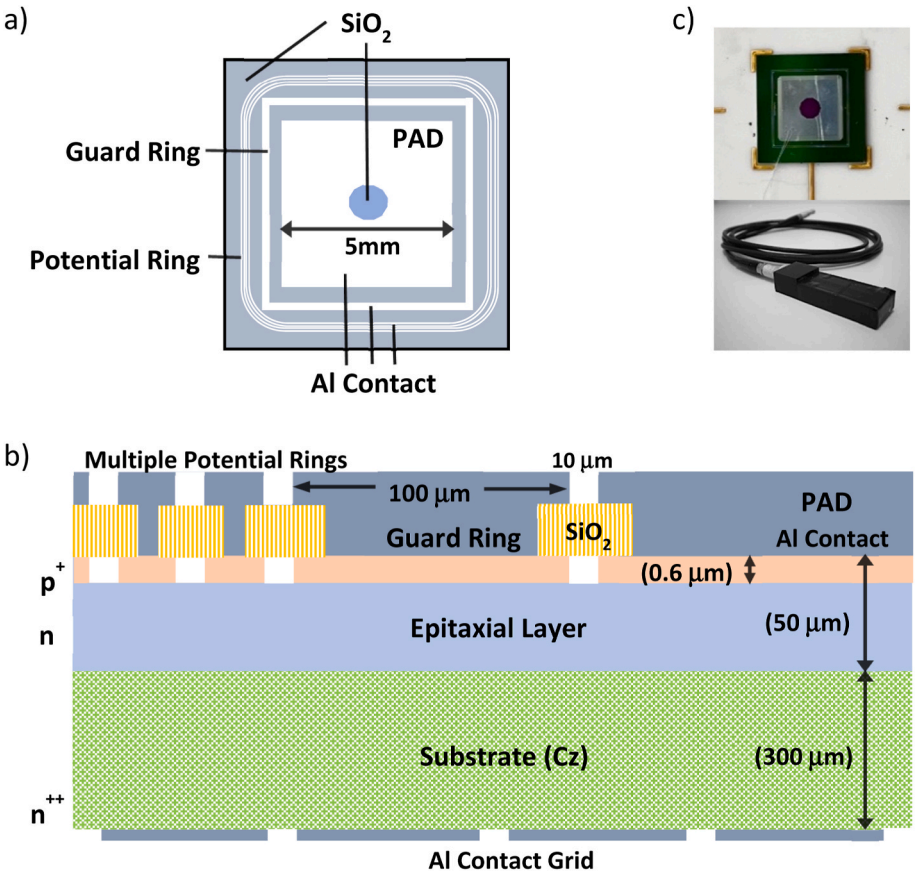

Fig. 1. - a) Top view of the epitaxial diode geometry used in this work; b) Schematic structure of the EPI diode with dimensions out of scale for easy visualization (Adapted from Junkes, 2011); c) photograph of the EPI diode and dosimetric probe.

et al., 2007). The pad is surrounded by a structure comprising a guard ring (100 μm wide) and a few thin potential rings arranged to smooth the potential drop between the guard ring and the outer region of the diode in case it is reversely biased. For clarity, Fig. 1a and b shows a top view of the diode geometry and its schematic structure with dimensions out of scale for easy visualization.

Five similar EPI diodes have been used in this work. They are electrically characterized (I-V curves) to assess the batch uniformity using a semiconductor device analyzer (Keithley, model SMU 2450). At room temperature (22 °C), all devices exhibit very low dark currents, 2.2 pA (0.05 mV) up to 9.8 nA (30 V).

To be employed as dosimeters, each device is fixed on a ceramic plate ($20 \times 25 \times 0.6\ mm^3$) using conductive epoxy paint and housed in a light-tight polymethylmethacrylate probe with an entrance window covered by a thin ($8.3\ mg/cm^2$) black paperboard (Fig. 1c). The planar pad (p^+) signal electrode is connected, through low-noise Lemo® coax cable, to the input of a Keithley® 6517B electrometer with the backplane n^{++} grounded and the guard ring structure floating. The current measurements are taken in the short-circuit mode without externally applied voltage to the diode.

2.2. Irradiation setups and ionization chambers

The dosimetric parameters are evaluated for radiation quality diagnostic radiology RQR-3, RQR-5, RQR-8, and RQR-10, and radiation quality computed tomography RQT-8, RQT-9, and RQT-10 beams established according to IEC 61267 (2005). Irradiations are performed with a Pantak-Seifert 160HS Isovolt X-ray generator previously standardized by Radcal RC6-RD and RC3-CT ionization chambers. Both chambers have been calibrated at the *Physikalisch-Technische Bundesanstalt* (PTB) with a standard deviation of 0.77% and 1.5%, respectively. Unless otherwise stated, each EPI diode used in this work is positioned at the center of a circular irradiation field of 12 cm diameter, with 99% homogeneity, at 100 cm from the X-ray tube (focal spot). A circular plane-parallel transmission ionization chamber, PTW® model 34014-0040, placed at the exit of the X-ray beam, monitors the irradiations with the diagnostic radiology and computed tomography beams qualities for reference. The air kerma rates and the main characteristics of the RQR and RQT beams are given in Table 1.

A small-scale ^{60}Co Gammacell-220 irradiator type I (Atomic Energy of Canada Limited) is also employed to investigate the radiation tolerance of EPI diodes and their expected dose lifespan. The facility is calibrated with standard reference alanine dosimeters (1.7%, k = 2) traceable to the secondary standard laboratory at the International Atomic Energy Agency (IAEA). Irradiations are performed at a dose rate of 335.96 Gy/h, enabling the achievement of accumulated doses up to 100 kGy.

2.3. Dose rate response

The dose rate response, i.e., the current reading as a function of the dose rate, is investigated for the reference RQR-5 and RQT-9 beam qualities. Variations in the dose rates between 6.8 mGy/min and 115.8 mGy/min are accomplished by changing the X-ray tube current (2 mA–30 mA). At each condition, the electrometer continuously acquires five consecutive irradiation cycles, corresponding to switching the beam on (60 s) and off (60 s). Leakage currents, acquired when the shutter is closed, enable the signal-to-noise ratio to be calculated.

Table 1
Characteristics of radiation quality diagnostic radiology (RQR) and radiation quality computed tomography (RQT) beams from Pantak-Seifert 160HS Isovolt generator.

Diagnostic Radiology				
Quality	kV	mA	Filter (mm)	Air Kerma Rate (mGy/min)
RQR-3	50	10	2.40 Al	22.4 ± 0.2
RQR-5	70	10	2.80 Al	38.6 ± 0.3
RQR-8	100	10	3.20 Al	69.3 ± 0.5
RQR-10	150	10	4.20 Al	120 ± 0.2
Computed Tomography				
RQT-8	100	10	3.2 Al + 0.30 Cu	22.0 ± 0.7
RQT-9	120	10	3.5 Al + 0.35 Cu	34.0 ± 0.1
RQT-10	150	10	4.2 Al + 0.35 Cu	57.0 ± 0.2

2.4. Repeatability parameter

The repeatability of the current signals is quantified for the reference RQR-5 and RQT-9 beams. Ten consecutive current signals, each lasting 60 s followed by a pause of 60 s, are taken for both beam qualities. Almost 120 acquisitions are performed during each irradiation cycle, and are, afterward, averaged to obtain the mean current. The coefficient of variation (CV) of each set of current readings, defined as the standard deviation expressed as a percentage of the mean value (IEC 61674, 2012), gives the repeatability parameter.

2.5. Long-term stability

The long-term stability of the response is assessed over one semester by monthly irradiating the diode with RQR-5 and RQT-9 beams under the same reference conditions regarding positioning, exposure time (five consecutive current signals, each lasting 60 s followed by a pause of 60 s), and dose rate (38.6 mGy/min for RQR-5 and 34 mGy/min for RQT-9). In each irradiation step, the output current value is the average of five consecutive readings. Between each set of measurements, all diodes are kept in a non-vacuum glass desiccator to prevent them from moisture and excessive temperature variations.

2.6. Angular dependence

The directional response is investigated for the reference RQR-5 beam by manually rotating the dosimetric probe, coupled to a commercial goniometer (Optron®, model GN1 200) with a resolution of 1°, from −5° to 5°, to adhere to the IEC 61674 (2012) standard. At each position, five consecutive current signals are recorded for 60 s at a constant dose rate (38.6 mGy/min). The data on the averaged currents are normalized to unity at the incidence angle of 0° when the beam hits the front surface of the diode perpendicularly.

2.7. Dose response

The dose response of the EPI diode, given by the charge produced in its sensitive volume as a function of the absorbed dose, is evaluated for all X-ray beam qualities covering doses up to 1.2 Gy. The main dosimetric features regarding linearity and the corresponding charge sensitivity, given by the slope of the linear plot, are also investigated. The energy dependence is assessed through the variations in the charge sensitivity values gathered with all the beam qualities.

The dependence on the average dose rate is checked by irradiating the diode at a constant dose (20 mGy) under 6.8 mGy/min and 115.8 mGy/min dose rates. Variations in the charges compared to those gathered with the reference RQR-5 and RQT-9 qualities are used as a parameter to infer the dose rate effect on the dose response.

2.8. Accumulated dose stability

The radiation tolerance of the diode is indirectly assessed through variations in the output currents measured before any radiation damage and those acquired after accumulating doses high enough to onset detectable current changes. Ideally, to achieve such doses (at least a few tents of Gy), the diode should be continuously irradiated with diagnostic radiology and computed tomography beams, which is time-consuming and practically unfeasible with an X-ray generator. For this reason,

fractioned irradiations are performed with ^{60}Co gamma rays covering doses between 10 Gy and 100 kGy at 335.96 Gy/h. After each gamma irradiation cycle, the diode is irradiated with the RQR-5 and RQT-9 beams under the same reference conditions cited in Section 2.2. Five output currents are consecutively recorded for both beam qualities to improve the data accuracy and evaluate the repeatability parameter following the same procedure described in Section 2.3 for the pristine (non-previously irradiated) diode.

The accumulated dose stability parameter, given by the ratio of the percentage change in current per accumulated dose, is experimentally assessed through the current sensitivity variation, compared to that obtained with the pristine diode, as a function of the accumulated doses. Such data are useful to predict the lifespan of the diode, that is, the maximum dose it can withstand while still meeting the performance requirements of the accumulated dose stability according to IEC 61674 (2012).

2.9. Combined uncertainties of the dosimetric parameters and compliance with dosimetry standards

The technical procedures adopted for measuring the dosimetric parameters are bound to comply with internationally accepted recommendations for diode-based dosimeters in medical dosimetry (IEC 61674, 2012). To fulfill the requirements of the IEC 61674 norm, all measurements are performed at constant room temperature (20 °C) and air humidity (50%).

The combined uncertainty of each performance characteristic is assessed by adding all the components (types A and B) of the standard uncertainties in quadrature (JCGM 100, 2008). The combined uncertainties of the results are due to the standardized ionization chambers (0.77% and 1.5%), electrometer precision (0.2%), source-detector distance (0.05%). goniometer (0.05%), chronometer (0.004%), and thermometer (0.01%). The combined uncertainties are expanded to k = 2 (confidence level of 95%). In all figures, the experimental values are plotted with the respective error bars, which are sometimes not visible when smaller than the size of the symbols.

3. Results

3.1. Dose rate response

Fig. 2 exhibits the linear dose rate response for RQR-5 and RQT-9 covering the air kerma rate range between 6.8 mGy/min and 115.8 mGy/min. Variations in air kerma rates are accomplished by changing the X-ray tube current from 2 mA to 30 mA. The current sensitivities, assessed through the slope of each linear plot, are (0.206 ± 0.003) nA min/mGy (RQR-5) and (0.138 ± 0.003) nA min/mGy (RQT-9).

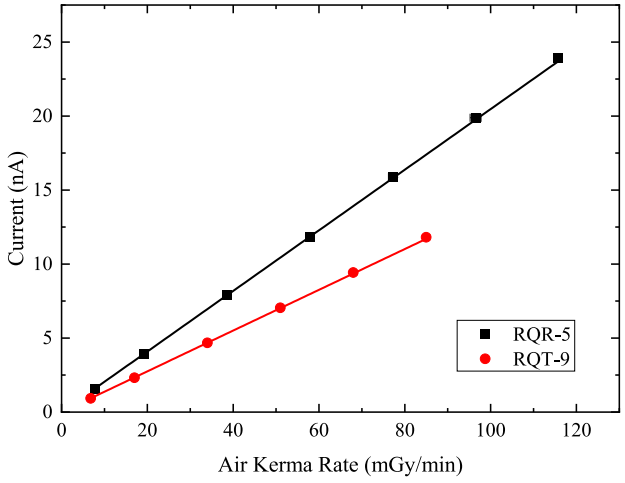

Fig. 2. Dose rate responses of the EPI diode irradiated with RQR-5 and RQT-9 beams. The overall uncertainties are 0.8% (RQR-5) and 1.6% (RQT-9).

3.2. Repeatability

Fig. 3 shows the output current signals from a pristine diode consecutively irradiated with RQR-5 (38.6 mGy/min) and RQT-9 (34.0 mGy/min) beams. It depicts stable current signals with currents almost four orders of magnitude higher than the leakage ones recorded with the shutter closed. To infer the effect of the leakage current on the current signal, the first set of current readings (Fig. 3a) is plotted again on a logarithmic scale in Fig. 3b. Despite the inaccuracy of such low leakage current measurements, the current signal-to-noise ratio (SNR), estimated through the ratio between the averaged current signal acquired at each dose rate and the standard deviation of the leakage current, is about 9900 (RQR-5) and 4900 (RQT-9), well above that recommended (10^3) for ionization chambers (IEC 61674, 2012).

3.3. Long-term stability

The residues of the current readings from the average value of the measurements gathered for RDR-5 and RQT-9 qualities are depicted in Fig. 4. Each data point is the average of three measurements monthly performed throughout a semester. Using linear regression analysis, these readings are extrapolated to obtain the current response change over one full year. The high long-term stability of the current response, better than 0.4%/year, complies with the requirement (≤1%/year) of the IEC 61674 (2012) standard.

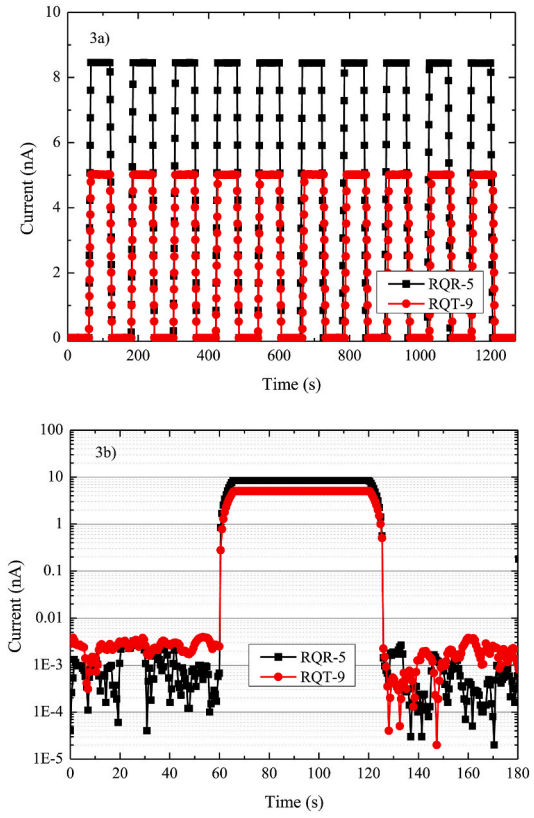

Fig. 3. - a) Current signals from a pristine diode consecutively irradiated with RQR-5 (38.6 mGy/min) and RQT-9 (34 mGy/min) beams; b) Current signal profiles plotted in logarithmic scale to infer the leakage current (shutter closed) effect on the radiation-induced current. The overall experimental uncertainties are 0.8% (RQR-5) and 1.6% (RQT-9).

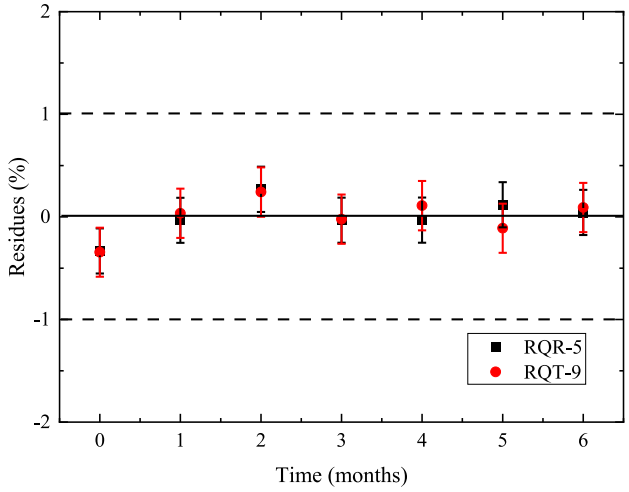

Fig. 4. - Residues of the current data from the average values of the measurements gathered for RQR-5 and RQT-9 beam qualities. The error bars correspond to the propagation of the instrumental and statistical uncertainties of each current reading (except the ionization chamber errors). The dashed lines represent the maximum current variation (1%) recommended by the IEC 61674 standard.

3.4. Angular dependence

The angular (or directional) dependence of the diode response, evaluated for the reference diagnostic radiology RQR-5 beam, is shown in Fig. 5. Each point is the average of five current readings normalized to unity at an incidence angle of 0° (normal incidence to the surface of the diode). The current intensity decreases when it is rotated by ± 5° from the normal incidence regardless of the rotation direction. In oblique incidences, the beam travels a greater distance before reaching the sensitive volume of the diode and, therefore, is more attenuated in the entrance windows of the probe (8.3 mg/cm^2) and the diode (0.14 mg/cm^2). In this case, the directional response is affected by the structural characteristics of the diode and its assembly on the probe. Despite this experimental limitation and even for the lowest beam energy (RQR-5), the response variation of less than 3% within an angular range of ± 5° still adheres to the IEC 61674 requirements. The directional response of the EPI diode enables its application in the dosimetry procedures involving rotational treatments.

3.5. Dose response and sensitivity

The dose response of the EPI diode is evaluated by plotting the charge (obtained by integrating the current signals) as a function of the accumulated dose for the diagnostic radiology beam qualities at the air kerma rates presented in Table 1. The data sets in Fig. 6 are well-fitted by a linear function (correlation coefficients $R^2 \cong 0.999$), and are characterized by charge sensitivities slightly dependent on the beam energy. This effect is most evident for the computed tomography beams shown in Fig. 7, where charge sensitivity discrepancies to the reference RQT-9 beam reach 10%. Physically, these sensitivity discrepancies are related to the variation in the diode response with the beam energy, depending on its physical and structural characteristics. As the active layer of the diode is reduced to the epitaxial layer (50 μm), the energy deposited by the diagnostic radiology and computed tomography beams, within the range from 50 kV to 150 kV, can vary significantly. This hypothesis is endorsed by the data presented in Table 2, illustrating the good agreement for the charge sensitivities obtained with the RQR-10 and RQT-8 beams, both with similar mean energies.

The dependence of the dose response on the dose rate is investigated by irradiating the diode to 20 mGy at different dose rates. Fig. 8 shows the residues of each charge value from the average of the whole data set gathered with RQR-5 and RQT-9 beam qualities. These results reveal a dose rate effect better than 2%, within the limits of variation (±2%) of this performance characteristic recommended by IEC 61674 (2012).

3.6. Accumulated dose stability

Fig. 9 shows the current variation as a function of the accumulated dose between 10 Gy and 100 kGy, for the two reference beams (RQR-5 and RQT-9). Each data point is the average of five consecutive current readings. Independently of the accumulated doses and beam qualities, all current signals are stable, with CV better than 0.3%.

The data set is normalized to the current acquired with the pristine diode irradiated with the reference RQR-5 and RQT-9 beams, respectively. The sensitivity drop profile, with a fast drop at the beginning of the irradiation followed by a slower one for higher doses, is typical of the induced radiation damage effects. This decay, about 1.5% even for accumulated doses of almost 40 Gy, does not adhere to the IEC 61674 (2012) requirements for the stability of the accumulated dose (1%/40 Gy). The issue is evidenced in the inset plot in Fig. 9, where an expanded view of the normalized current decay with accumulated doses up to 50 Gy is shown. However, for doses of 20 kGy upward, the relative decrease

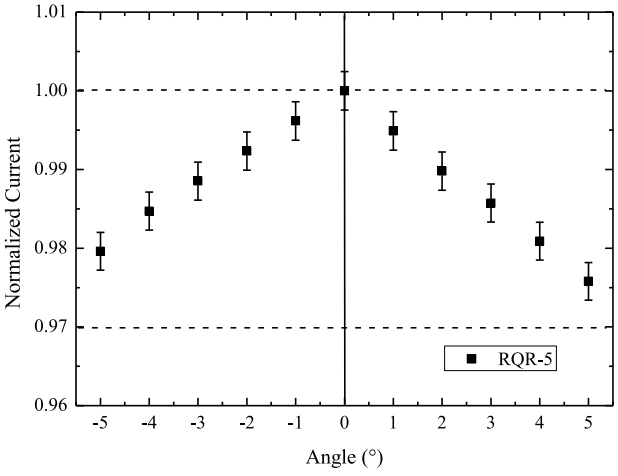

Fig. 5. Directional response of the EPI diode for RQR-5 beam quality. The dashed lines show the maximum variation (≤3% within an angle range of ± 5°) required by the IEC 61674 (2012).

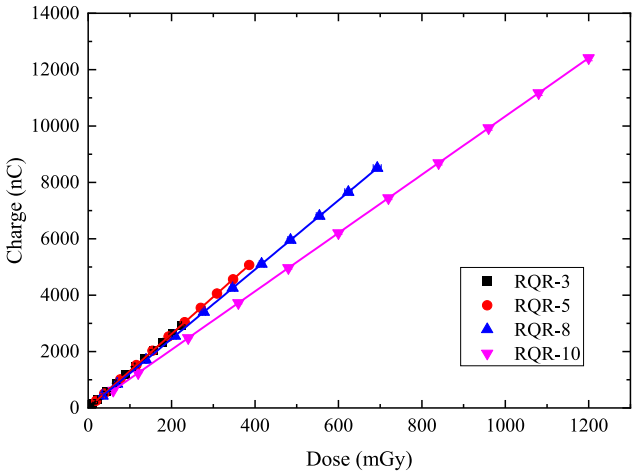

Fig. 6. Dose response of the EPI diode for RQR-3, RQR-5, RQR-8, and RQR-10 beam qualities. The corresponding charge sensitivities RQR-3/5/8 agree within 5%. The maximum experimental uncertainty is 0.8%.

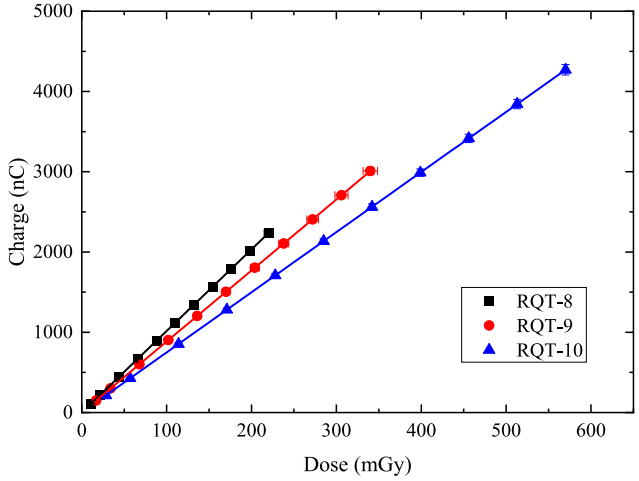

Fig. 7. Dose response of the EPI diode for RQT-8, RQT-9, and RQT-10 beam qualities with a maximum experimental uncertainty of 1.6%. The discrepancies of the charge sensitivities among all the RQT qualities are greater than 10%.

Table 2
Charge Sensitivities of the diagnostic radiology and computed tomography beams from the Pantak-Seifert 160HS Isovolt generator.

Quality	kV	mA	Mean Energy (keV)	Charge Sensitivity (μC/Gy)
RQR-3	50	10	31.9	13.06 ± 0.15
RQR-5	70	10	39.5	13.13 ± 0.15
RQR-8	100	10	49.6	12.28 ± 0.14
RQR-10	150	10	62.9	10.35 ± 0.12
RQT-8	100	10	60.6	10.16 ± 0.22
RQT-9	120	10	67.4	8.85 ± 0.19
RQT-10	150	10	75.2	7.49 ± 0.17

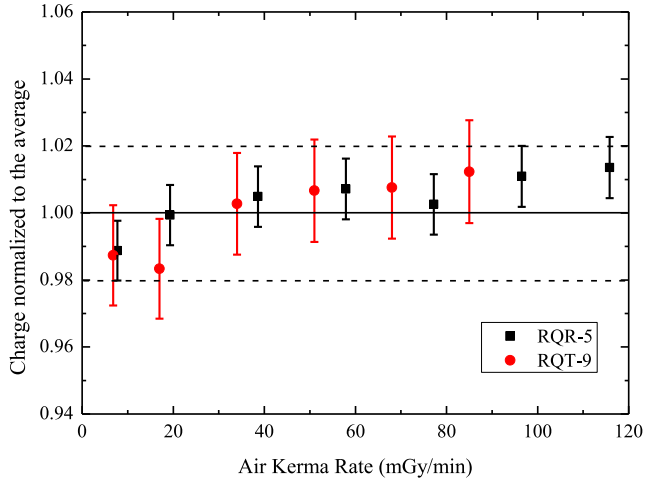

Fig. 8. Dose-response dependence on the dose rate between 6.8 mGy/min and 115.8 mGy/min for the RQR-5 and RQT-10 qualities. For each dose rate, the diode is irradiated at 20 mGy. The dashed lines represent the limits of the dose rate dependence recommended by the IEC 61674 norm.

in the current sensitivity slowly tends to saturation. Better response stability is found with the diode pre-irradiated with doses from 30 kGy up to 70 kGy, as illustrated in Fig. 10. The plot shows that the higher the preirradiated dose, the less the current decays with increasing accumulated doses. Furthermore, the accumulated dose stability condition

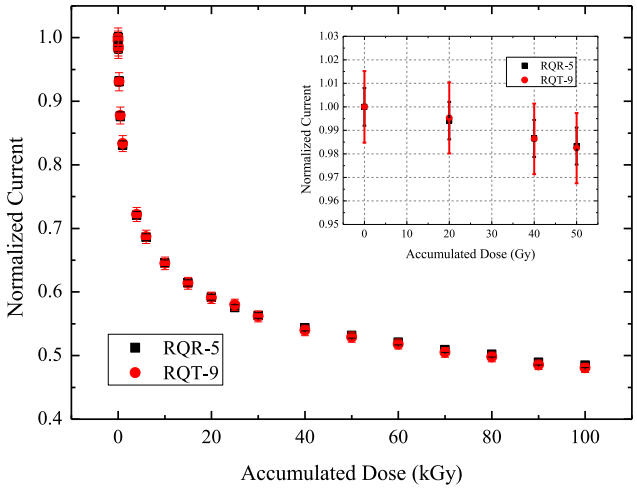

Fig. 9. Normalized current decay with increasing absorbed doses up to 100 kGy for the RQR-5 and RQT-9 beams. The inset plot shows an expanded view of the current decay for doses lower than 50 Gy.

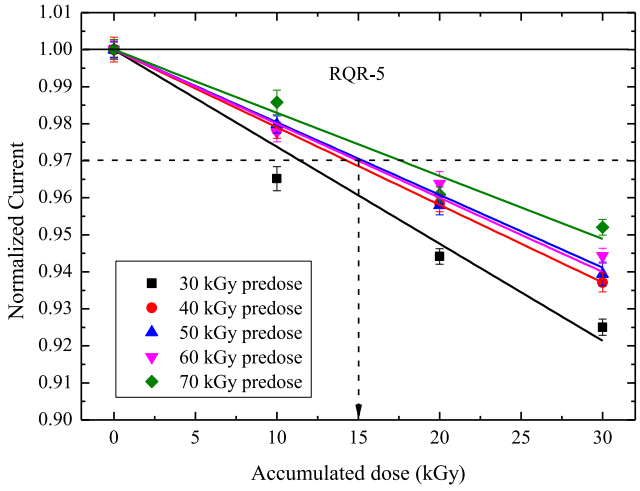

Fig. 10. Normalized current decay of the diode preirradiated to different pre-irradiation doses obtained with the RQR-5 beam quality. The dashed lines represent the limit of 3% stipulated in the IEC 61674 requirements for dose stability.

(1%/40 Gy) is satisfied for the whole range of predoses despite a slight dependence of the accumulated doses on the current sensitivity. Fig. 10 also reveals that the predose of about 50 kGy is the one that best satisfies the balance between greater stability and a reasonable response sensitivity. The diode lifespan, the maximum dose it withstands for dosimetric response variations less than 3%, is graphically inferred from the data sets in Fig. 10 as almost 15 kGy. It is well above what is necessary in diagnostic radiology and computed tomography dosimetry.

4. Discussion

The response of a custom-made dosimetry system based on a rad-hard EPI diode is fully evaluated for diagnostic radiology and computed tomography beams. The dosimetric parameters of repeatability (<0.3%), long-term stability (0.4%/year), angular response (<3%, ± 5°), dose rate dependence (<3%), and signal-to-noise ratio (≥4900) meet the requirements of the IEC 61674 (2012) norm. Regarding the dose response, the linearity between charge and dose is

evidenced in all data sets despite a nonnegligible energy dependence. It is demonstrated by the variations in the charge sensitivity of the diode irradiated with different X-ray beam qualities, as shown in Table 2. However, the variation in the response to different radiation qualities does not prevent the EPI diode from being used for CT dosimetry, provided it is calibrated against a standard ionization chamber to access the calibration coefficient for each RQT quality in accordance with TRS 457 (2007) recommendations.

Investigations of the radiation damage effects on the diode evidenced a current sensitivity drop of 1% when it accumulates 20 Gy. Despite the small doses encompassed in DR and CT beam dosimetry, which would guarantee the high reusability of this diode before requiring recalibrations, the dose of 20 Gy is negligible when compared to accumulated doses reported in the literature for fully depleted EPI diodes (Lindström et al., 1999, 2006). The difference originates from the physical phenomena underlying charge collection in a fully reversely polarized diode, i.e., drift current collected in a constant sensitive volume, and a non-externally polarized one, i.e., predominant diffusion current with possible volume variation. In the short-circuit mode of operation, the active volume is mostly determined by the minority carrier diffusion length, which varies with increasing accumulated doses. Theoretical support for this result is underway through simulations of the diffusion currents generated at the abrupt junction of the p^+ and n-type thin EPI layers deposited on a thick MCz substrate.

5. Conclusions

An EPI diode-based dosimetry system is thoroughly characterized in this work. The dose rate and dose responses for diagnostic radiology and computed tomography beams are linear despite a slight energy dependence. The dosimetric parameters regarding repeatability, long-term stability, angular response, dose rate dependence, and signal-to-noise ratio fully adhere to the IEC 61674 norm. Compliance with the accumulated dose stability requirement (1.0%/40 Gy) is almost achieved with the pristine diode and effectively accomplished through radiation conditioning with ^{60}Co gamma rays. Under the latter condition, the lifespan of the diode can easily reach 15 kGy, assuring the high reusability of this diode for diagnostic radiology and computed tomography dosimetry before requiring recalibrations. Such good results endorse using the EPI diodes as a reliable dosimeter for diagnostic radiology and computed tomography dosimetry.

CRediT authorship contribution statement

JosemaryA.C. Gonçalves: Writing – review & editing, Resources, Methodology, Investigation, Funding acquisition, Formal analysis, Data curation. **Alessio Mangiarotti:** Writing – review & editing, Methodology, Formal analysis. **Patrícia L. Antonio:** Investigation, Data curation. **LindaV.E. Caldas:** Writing – review & editing, Funding acquisition. **CarmenC. Bueno:** Writing – review & editing, Writing – original draft, Supervision, Methodology, Formal analysis, Conceptualization.

Declaration of competing interest

The authors declare that they have no known competing financial interests or personal relationships that could have appeared to influence the work reported in this paper.

Data availability

Data will be made available on request.

Acknowledgments

The authors highly acknowledge Dr. I. Pintilie (Department of Semiconductor Physics and Complex Structures, National Institute of Materials Physics, Romania), G. Lindström, and E. Fretwurst (from the University of Hamburg, Germany) for the free diodes supply. The authors thank L. C. dos Santos (IPEN-CNEN/SP) for collaborating during the irradiation procedures. The authors also thank R. C. Teixeira (Electronic Packing staff) from Centro de Tecnologia da Informação Renato Archer (CTI-Renato Archer, Campinas/SP) for useful discussions and the measurements of I-V curves. This work is part of the Brazilian Institute of Science and Technology for Nuclear Instrumentation and Applications to Industry and Health (INCT/INAIS), CNPq project 406303/2022-3. FAPESP supports this work under contract nº 2018/05982-0 and 2022/13430-2, and CNPq under process number 305142/2021-6.

References

Aldosari, A.H., Espinoza, A., Robinson, D., Fuduli, I., Porumb, C., Alshaikh, S., Carolan, M., Lerch, M.L.F., Perevertaylo, V., Rosenfeld, A.B., Petasecca, M., 2013. Characterization of an innovative p-type epitaxial diode for dosimetry in modern external beam radiotherapy. IEEE Trans. Nucl. Sci. 60 (6), 4705–4712. https://doi.org/10.1109/TNS.2013.2289909.

Barthe, J., 2001. Electronic dosimeters based on solid state detectors. Nucl. Instrum. Methods B 184, 158–189. https://doi.org/10.1016/S0168-583X(01)00711-X.

Bruzzi, M., Bucciolini, M., Casati, M., Menichelli, D., Talamonti, C., Piemonte, C., Svensson, B.G., 2007. Epitaxial silicon devices for dosimetry applications. Appl. Phys. Lett. 90, 172109–172111. https://doi.org/10.1063/1.2723075.

Bueno, C.C., Camargo, F., Gonçalves, J.A.C., Pascoalino, K., Mangiarotti, A., Tuominen, E., Härkönen, J., 2022. Performance characterization of dosimeters based on radiation-hard silicon diodes in gamma radiation processing. Front. Sens. 3, 770482–770492. https://doi.org/10.3389/fsens.2022.770482.

Camargo, F., Khoury, H.J., Nascimento, C.R., Asfora, V.K., Bueno, C.C., 2007. Evaluation of a multi-guard ring (MGR) structure diode as diagnostic X-ray dosimeter. Nucl. Instrum. Methods Phys. Res., Sect. A 580, 194–196. https://doi.org/10.1016/j.nima.2007.05.082.

Candelori, A., 2006. Radiation-hard detectors for very high luminosity colliders. Nucl. Instrum. Methods Phys. Res., Sect. A 560 (1), 103–107. https://doi.org/10.1016/j.nima.2005.11.250.

Casati, M., Bruzzi, M., Bucciolini, M., Menichelli, D., Scaringella, M., Piemonte, C., Fretwurst, E., 2005. Characterization of standard and oxygenated float zone Si diodes under radiotherapy beams. Nucl. Instrum. Methods Phys. Res., Sect. A 552 (1–2), 158–162. https://doi.org/10.1016/j.nima.2005.06.025.

Damulira, E., Yusoff, M.N.S., Omar, A.F., Taib, N.H.M., 2019. A review: photonic devices used for dosimetry in medical radiation. Sensors 19, 2226–2254. https://doi.org/10.3390/s19102226.

Fretwurst, E., Hönniger, F., Kramberger, G., Lindström, G., Pintilie, I., Röder, R., 2007. Radiation damage studies on MCz and standard and oxygen enriched epitaxial silicon devices. Nucl. Instrum. Methods Phys. Res., Sect. A 583 (1), 58–63. https://doi.org/10.1016/j.nima.2007.08.194.

Gonçalves, J.A.C., Pereira, L.N., Potiens, M.P.A., Vivolo, V., Bueno, C.C., 2014. Evaluation of epitaxial silicon diodes as dosimeters in X-ray mammography. Radiat. Meas. 71, 384–388. https://doi.org/10.1016/j.radmeas.2014.07.014.

Gonçalves, J.A.C., Mangiarotti, A., Bueno, C.C., 2020. Current response stability of a commercial PIN photodiode for low-dose radiation processing applications. Radiat. Phys. Chem. 167, 108276–108279. https://doi.org/10.1016/j.radphyschem.2019.04.026.

Gonçalves, J.A.C., Mangiarotti, A., Asfora, V.K., Khoury, H.J., Bueno, C.C., 2021. The response of low-cost photodiodes for dosimetry in electron beam processing. Radiat. Phys. Chem. 181, 109335–109342. https://doi.org/10.1016/j.radphyschem.2020.109335.

Gonçalves, J.A.C., Mangiarotti, A., Bueno, C.C., 2022. Characterization of a thin photodiode as a routine dosimeter for low-dose radiation processing applications. Radiat. Phys. Chem. 198, 110200–110206. https://doi.org/10.1016/j.radphyschem.2022.110200.

Griessbach, I., Lapp, M., Bohsung, J., Gademann, G., Harder, D., 2005. Dosimetric characteristics of a new unshielded silicon diode and its application in clinical photon and electron beams. Med. Phys. 32 (12), 3750–3754. https://doi.org/10.1118/1.2124547.

Grusell, E., Medin, J., 2000. General characteristics of the use of silicon diode detectors for clinical dosimetry in proton beams. Phys. Med. Biol. 45, 2573–2582. https://doi.org/10.1088/0031-9155/45/9/310.

Härkönen, J., Tuovinen, E., Luukka, P., Nordlund, H.K., Tuominen, E., 2007. Magnetic Czochralski silicon as detector material. Nucl. Instrum. Methods Phys. Res., Sect. A 579 (2), 648–652. https://doi.org/10.1016/j.nima.2007.05.264.

Hönniger, F., Fretwurst, E., Lindström, G., Kramberger, G., Pintilie, I., Röder, R., 2007. DLTS measurements of radiation-induced defects in epitaxial and MCZ silicon detectors. Nucl. Instrum. Methods Phys. Res., Sect. A 583 (1), 104–108. https://doi.org/10.1016/j.nima.2007.08.202.

IEC 61267, 2005. International Electrotechnical Commission, Medical Diagnostic X-Ray Equipment - Radiation Conditions for Use in the Determination of Characteristics, second ed.

IEC 61674, 2012. International Electrotechnical Commission, Medical Electrical Equipment - Dosimeters with Ionization Chambers And/or Semiconductor Detectors as Used in X-Ray Diagnostic Imaging, second ed.

JCGM 100, 2008. BIPM, IEC, IFCC, ILAC, ISO, IUPAC, IUPAP, and OIML. Evalu- ation of measurement data - guide to the expression of uncertainty in measurement. Joint Committee for Guides in Metrology. JCGM 100, 2008.

Junkes, A., 2011. Influence of Radiation Induced Defect Clusters on Silicon Particle Detectors. University of Hamburg. PhD Thesis, Department of Physics.

Jursinic, P., 2019. PIN diodes for radiation therapy use: their construction, characterization, and implementation. Phys. Med. 59, 86–91. https://doi.org/10.1016/j.ejmp.2019.02.021.

Jursinic, P., 2023. A PIN photodiode ionizing radiation detector with small angular dependence and low buildup. Radiat. Meas. 166, 106963–106968. https://doi.org/10.1016/j.radmeas.2023.106963.

Kemmer, J., Wiest, F., Pahlke, A., Boslau, O., Goldstrass, P., Eggert, T., Schindler, M., Eisele, I., 2005. Epitaxy - a new technology for the fabrication of advanced silicon radiation detectors. Nucl. Instrum. Methods Phys. Res., Sect. A 544 (3), 612–619. https://doi.org/10.1016/j.nima.2005.02.013.

Khoury, H.J., Hazin, C.A., Mascarenhas, A.P., da Silva Jr, E.F., 1999. Low-cost silicon photodiode for electron dosimetry. Radiat. Protect. Dosim. 84 (1–4), 341–343. https://doi.org/10.1093/oxfordjournals.rpd.a032751.

Kumar, R., Sharma, S.D., Philomina, A., Topkar, A., 2014. Dosimetric characteristics of a PIN diode for radiotherapy application. Technol. Cancer Res. Treat. 13 (4), 361–367. https://doi.org/10.7785/tcrt.2012.500388.

Liao, C., Fretwurst, E., Garutti, E., Schwandt, J., Pintilie, I., Nitescu, A., Himmerlich, A., Moll, M., Gurimskaya, Y., Li, Z., 2024. Investigation of high resistivity p-type FZ silicon diodes after ^{60}Co γ-irradiation. Nucl. Instrum. Methods Phys. Res., Sect. A 1061, 169103. https://doi.org/10.1016/j.nima.2024.169103.

Lindström, G., Moll, M., Fretwurst, E., 1999. Radiation hardness of silicon detectors – a challenge from high-energy physics. Nucl. Instrum. Methods Phys. Res., Sect. A 426 (1), 1–15. https://doi.org/10.1016/S0168-9002(98)01462-4.

Lindström, G., Dolenc, I., Fretwurst, E., Hönniger, F., Kramberger, G., Moll, M., Nossarzewska, E., Pintilie, I., Röder, R., 2006. Epitaxial silicon detectors for particle tracking – radiation tolerance at extreme hadron fluencies. Nucl. Instrum. Methods Phys. Res., Sect. A 568 (1), 66–71. https://doi.org/10.1016/j.nima.2006.05.203.

Moll, M., 2018. Displacement damage in silicon detectors for high energy physics. IEEE Trans. Nucl. Sci. 65 (8), 1561–1582. https://doi.org/10.1109/TNS.2018.2819506.

Oliveira, C.N.P., Khoury, H.J., Santos, E.J.P., 2016. PIN photodiode performance comparison for dosimetry in radiology applications. Phys. Med. 32, 1495–1501. https://doi.org/10.1016/j.ejmp.2016.10.018.

Pettinato, S., Girolami, M., Stravato, A., Serpente, V., Musio, D., Rossi, M.C., Trucchi, D. M., Olivieri, R., Salvatori, S., 2023. A highly versatile X-ray and electron beam diamond dosimeter for radiation therapy and protection. Materials 16 (2), 824–834. https://doi.org/10.3390/ma16020824.

Pini, S., Bruzzi, M., Bucciolini, M., Borchi, E., Lagomarsino, S., Menichelli, D., Miglio, S., Nava, F., Sciortino, S., 2003. High-bandgap semiconductor dosimeters for radiotherapy applications. Nucl. Instrum. Methods A. 514 (1–3), 135–140. https://doi.org/10.1016/j.nima.2003.08.095.

Rikner, G., Grussel, E., 1983. Effects of radiation damage on p-type silicon detectors. Phys. Med. Biol. 28, 1261–1267. https://doi.org/10.1088/0031-9155/28/11/006.

Rosenfeld, A.B., 2002. MOSFET dosimetry on modern radiation oncology modalities. Radiat. Protect. Dosim. 101 (1–4), 393–398. https://doi.org/10.1093/oxfordjournals.rpd.a006009.

Rosenfeld, A.B., 2007. Electronic dosimetry in radiation therapy. Radiat. Meas. 41 (Suppl. 1), S134–S153. https://doi.org/10.1016/j.radmeas.2007.01.005.

Rosenfeld, A.B., 2016. Novel detectors for silicon based microdosimetry, their concepts and applications. Nucl. Instrum. Methods A 809, 156–170. https://doi.org/10.1016/j.nima.2015.08.059.

Santos, T. C. dos, Neves-Junior, W.F.P., Gonçalves, J.A.C., Haddad, C.M.K., Bueno, C.C., 2011. Evaluation of rad-hard epitaxial silicon diode in radiotherapy electron beam dosimetry. Radiat. Meas. 46 (12), 1662–1665. https://doi.org/10.1016/j.radmeas.2011.05.064.

TRS 457, 2007. Technical Reports Series, Dosimetry in Diagnostic Radiology : an International Code of Practice. International Atomic Energy Agency.